Methodology

Diallyl disulfide, a garlic-rich compound ameliorates trichloromethane-induced renal oxidative stress, NFkB activation and apoptosis in rats

Oluwatobi T. Somade[*], Adeyinka H. Adedokun, Idowu K. Adeleke, Muslimot A. Taiwo, Mulikat O. Oyeniran

Department of Biochemistry, College of Biosciences, Federal University of Agriculture Abeokuta, Nigeria

A R T I C L E   I N F O

S U M M A R Y

The renal-protective effect of diallyl disulfide (DADS) on tricholoromethane ($CHCl_3$)-induced renal toxicity was investigated. Twenty five rats, divided into five groups of five animals each were used. $CHCl_3$ at the dose of 200 mg/kg was orally administered, and concomitantly treated with DADS (50 mg/kg), 5 days/week for a period of 3 weeks. Compared with control, there was no significant increase in kidney malondialdehyde (MDA), but a significant increase in levels of nuclear factor kappa B (NFkB) expressions, TUNEL positive cells (apoptosis), as well as hydrogen peroxide (H_2O_2), nitric oxide (NO) and reduced glutathione (GSH) concentrations. In addition, a significant decrease in expressions of kidney p53 and catalase (CAT) activity, and a non-significant decrease in glutathione peroxidase (GPx) activity were recorded following $CHCl_3$ administration. Conversely, following DADS treatment, there was a significant increase in the expressions of p53, and a significant and non-significant decrease in apoptotic positive cells and NFkB expressions respectively. Administration of DADS significantly reduced the levels of H_2O_2 and NO, but did not have effect on the level of GSH, while CAT and GPx activities were significant improved. Protection by DADS against TCM-induced renal-toxicity

* Corresponding author. Department of Biochemistry, College of Biosciences, Federal University of Agriculture Abeokuta, Nigeria.
   E-mail address: toblerum@yahoo.co.uk (O.T. Somade).

may therefore be via suppressions of NFkB activation, oxidative stress and apoptosis in rats.

1. Introduction

$CHCl_3$ is a colorless and volatile liquid with a distinct odor. $CHCl_3$ is nonflammable, slightly soluble in water and is readily miscible with most organic solvents [1]. $CHCl_3$ is the most predominant by-product of water disinfection with chlorine-based chemicals [2], also formed in large quantities as a consequence of chlorination of cooling water in power plants and in the process of bleaching paper [3]. $CHCl_3$ has a widespread use in industry as solubilizer, diluent, and dispersant [4]. It is one of the major environmental toxicants [5], classified as a group 2B carcinogen [6]. At low concentrations, metabolism occurs majorly through cytochrome P_{450}-2E1 [7]. The level of P_{450}-2E1, and hence the rate of chloroform metabolism, is induced by a variety of alcohols such as ketones and ethanol. Also at high chloroform concentrations, metabolism is via cytochrome P_{450}–2B1/2 [8–10].

In the presence of oxygen, the predominant product is trichloromethanol, which spontaneously and effectively dehydrochlorinates to form phosgene. In the absence of oxygen, the major metabolite is dichloromethyl free radical [8,9]. Virtually all tissues of the body have capacity to metabolize $CHCl_3$, but the metabolic rate is greatest in kidney cortex, liver, and nasal mucosa [8]. These tissues are also the major sites of $CHCl_3$ toxicity, pointing the importance of metabolism in the mode of action of $CHCl_3$ toxicity.

Phosgene and dichloromethyl free radical, the products of oxidative metabolism and reductive metabolism respectively, are both highly reactive. The rate of phosgene hydrolysis is highly rapid, with a half-time of less than 1 s [11]. Phosgene also reacts with nucleophiles, including hydroxy groups, thiols, primary and secondary amines [12]. For example, phosgene reacts with the thiol group of GSH, forming S-chloro-carbonyl glutathione, which in turn can either interact further with glutathione to form diglutathionyl dithiocarbonate, or form glutathione disulfide and carbon monoxide [8]. The major reaction is hydrolysis by water, forming carbon dioxide and hydrochloric acid.

Phosgene also undergoes attack by nucleophilic groups such as $-NH_2$, $-OH$, and $-SH$ in cellular macromolecules including the polar heads of phospholipids, proteins or enzymes, resulting in generation of covalent adducts [13–18]. These molecular adducts can interfere with molecular functions such as loss of enzyme activity, which may lead to loss of cellular activities and subsequently cell death [8,19].

Pharmacological properties of phytochemicals are well documented and their underlying mechanisms of action are gradually being understood. Garlic (*Allium sativum* L.) is one of the most used spices in food, and as remedy for a variety of illnesses [20]. In garlic, over 20 different kinds of organo-sulfur compounds have been identified from sulfur-containing amino acids, and are considered a cancer preventive agent. Previous studies have shown inhibition of chemically induced carcinogenesis in different organs by certain sulfur-containing compounds [21]. One of these compounds is DADS, a major component of the secondary metabolites that has been well documented as a potent compound to prevent cancer, urotoxicity, genotoxicity, nephrotoxicity, and hepatotoxicity [22–27].

DADS inhibits the promotion phase of DMBA-induced skin tumors in mice [28], the growth of canine mammary neoplastic CMT-13 cells [29], rat and human CYP2E1 and rat CYP2A3 expressions [30]. DADS affects histone acetylation and this may be attributed to its protective properties in colon cancer [31]. DADS induces apoptosis in neuroblastoma cells [32] and HepG2 hepatoma [33], suggesting it as an anti-proliferative agent in cancer therapy [32].

Evaluation of biochemical and molecular mechanism by which $CHCl_3$ causes renal toxicity in rats and the search for alternatives that ameliorate this toxicity may provide substantial information with clinical implications. Based on the aforementioned, the present study investigated the chemotherapeutic effects of DADS on $CHCl_3$-induced renal toxicity in male wistar rats.

2. Materials and methods

2.1. Chemicals and test substances

CHCl$_3$ (98% purity), is a product of AD Chemicals Limited, Great Britain. DADS (98% purity) was purchased from Sigma Chemical Co., Saint Louis, MO, USA. Rat NFkB and p53 monoclonal primary antibodies were purchased from ABCAM UK; rat monoclonal secondary antibodies were purchase from Dako (Agilent Technologies, USA). Promega DeadEnd™ Colorimetric TUNEL System, for detection of apoptosis in tissue sections was purchased from Promega Corporation (Madison, WI, USA). Pure (100%) cholesterol free Mazola corn oil is a product of ACH Food Companies, Inc., Memphis, TN, USA. All other chemicals and reagents were of analytical grade, products of Sigma Chemical Co., Saint Louis, MO, USA or BDH Chemical Ltd, Poole, England.

2.2. Experimental animals and study design

Twenty five (25) male wistar albino rats of an average weight of 150 g used for this study were obtained from the animal house of the College of Veterinary Medicine, Federal University of Agriculture, Abeokuta, Nigeria. They were housed in steel metal cages in the animal house of our department and were served food and water *ad libitum*. Permission to use the animals was approved by the Institution's Animal Ethical Committee. After 3 weeks of acclimatization, the rats were divided randomly into five groups of five animals each. Group I rats served as normal control and were fed food and water only, group II rats served as vehicle control and were administered corn oil, group III was administered 200 mg/kg TCM only [34], group IV was administered 200 mg/kg TCM and concomitantly treated with 50 mg/kg DADS [27], while group V was administered 50 mg/kg DADS only. All administrations were done orally.

2.3. Sample collections and preparations

Administrations lasted for fifteen (15) days (5 days/week for 3 weeks), and 24 h after, animals were sacrificed. They were handled and used in accordance with the international guide for the care and use of laboratory animals [35]. The right kidneys were harvested, washed in ice-cold saline (0.9% w/v) solution, blotted dry, weighed and then fixed in 10% phosphate buffered formalin for terminal deoxynucleotidyl transferase dUTP nick end labeling (*TUNEL*) assay, immunohistochemistry, and histopathology. The rest was suspended in ice-cold 0.1 M phosphate buffer (pH 7.4) for homogenization. Homogenization was followed by centrifugation at 5000 rpm for 10 min. The resulting supernatant was aliquoted into Eppendorf tubes and used for other biochemical analyses.

2.4. Kidney immunohistochemistry

This was performed as described by Ajayi et al. [36]. Poly-L-lysine charged slides were rehydrated in xylene as well as decreasing concentration of ethanol (100—50%). Heat-induced epitope retrieval was done in citrate buffer (pH 6.0) for 20 min followed by immersion in cold water for 10 min. The sections were marked with PAP pen and the endogenous peroxidase activities in the tissues were blocked with 5% hydrogen peroxide for 5 min in a dark cupboard. The sections were subsequently incubated overnight at 4 °C with anti-NFkB or anti-p53 primary monoclonal antibodies. The slides were thereafter washed with Tris buffer saline and further incubated with Horse-radish peroxidase labeled anti-rabbit monoclonal secondary antibodies (Dako, Agilent Technologies, US). Immune complexes were visualized using 0.05 percent 3, 3-diaminobenzidene (DAB), countered stained with hematoxylin and the slides were visualized under light microscope. The percentage of tissue stained positive cells was scored.

2.5. TUNEL assay

This was carried out based on the manufacturer's protocol (Promega DeadEnd™ Colorimetric TUNEL System). Briefly, paraffin embedded tissue sections were washed in xylene for 5 min, followed

by immersion in 100% ethanol for 5 min, rehydrated in decreasing concentrations of ethanol (100–50%) for 3 min, and washed by immersion in 0.85% sodium chloride and phosphate buffer saline (PBS) for 5 min each. Apoptosis was detected by fixing slides in 4% paraformaldehyde in PBS for 15 min, addition of protein K solution and incubation at room temperature for 10–30 min. Equilibration buffer was added to equilibrate at room temperature for 5–10 min, followed by addition of recombinant terminal deoxynucleotidyl transferase (rTdT) reaction mixture to the tissue sections on the slides and then incubated for 60 min at 37 °C. Reaction was stopped by immersion in 2X saline-sodium citrate (2X SSC) buffer for 15 min, blocked by immersion of slides in 0.3% hydrogen peroxide for 3–5 min. Streptavidin HRP was added to slides, incubated for 30 min at room temperature, stained with diaminobenzidine (DAB) and developed until a light brown background appeared. Visualization of stained slides was done using Nikon E100 light microscope (Novel Optics, NanJing, China) for apoptotic cells.

2.6. Estimation of MDA concentration

MDA concentration, a marker of lipid peroxidation (LPO) was determined by the method of Buege and Aust [37]. In this procedure, 0.1 mL of the supernatant was added to 2 mL of trichloroacetic acid–thiobarbituric acid–hydrochloric acid (TCA/ TBA/HCl) (1:1:1 ratio) reagent, boiled at 100 °C for 15 min, and allowed to cool. Flocculent materials were removed by centrifuging at 3000 rpm for 10 min. The supernatant was removed and the absorbance read at 532 nm against blank. MDA concentration was calculated using the molar extinction coefficient for MDA-TBA complex of $1.55 \times 10^6 \ M^{-1}cm^{-1}$.

2.7. Estimation of H_2O_2 level

H_2O_2 level was estimated according to the method of Wolff [38]. Reaction mixture contains 2.5 mL of buffer, 250 μL Ammonium ferrous sulfate, 100 μL sorbitol, 100 μL xylenol orange, 25 μL sulfuric acid, and 50 μL of the sample. The mixture was thoroughly mixed till it foamed, followed by incubation for 30 min at room temperature. The pale pink color developed was read against blank at 560 nm.

2.8. Estimation of NO level

NO concentration in kidney was estimated using Griess Reagent [39]. The reaction mixture was made up of 150 μL sulfanilamide, 100 μL distilled water and 50 μL of sample. The mixture was incubated for 10 min, and then addition of 150 μL N-naphthylethylenediamine, followed by incubation for another 10 min. The concentration of NO was measured at 540 nm.

2.9. Estimation of GSH concentration

Reduced glutathione (GSH) level was determined by the method of Moron et al. [40], where the color developed was read at 412 nm.

2.10. Determination of GPx activity

GPx activity was determined by the method of Rotruck et al. [41]. Color developed was read at 412 nm.

2.11. Estimation of CAT activity

Catalase (CAT) activity was determined by the method of Sinha [42]. The reaction mixture (1.5 mL) contained 0.01 M phosphate buffer, pH 7.0, tissue homogenate (0.1 mL) and 2M H_2O_2 (0.4 mL). The reaction was stopped by the addition of 2 mL dichromate-acetic acid reagent (5% potassium

dichromate and glacial acetic acid mixed in 1:3 ratios), followed by heating in boiling water for 10 min, and then cooled at room temperature. The absorbance was read at 570 nm.

2.12. Determination of total protein concentration

Kidney total protein concentration was determined by the method of Gornall et al. [43], and used for the estimations of CAT and GPx activities.

2.13. Histopathological analysis

Briefly, kidney sections were fixed in phosphate buffered formaline solution for 48 h. After dehydration in an increasing concentration of alcohol and cleared twice in xylene, the tissues were embedded in paraffin, cut into sections, stained with haematoxylin–eosin dye, and finally observed at x 400 magnification under a Nikon light microscope.

2.14. Statistical analysis

Data were analyzed by one-way analysis of variance (ANOVA), followed by least significant difference (LSD) to test for significant differences among the groups of rats using Statistical Package for Social Sciences program version 17.0. Data were expressed as mean ± standard error of mean. P values less than 0.05 were considered statistically significant.

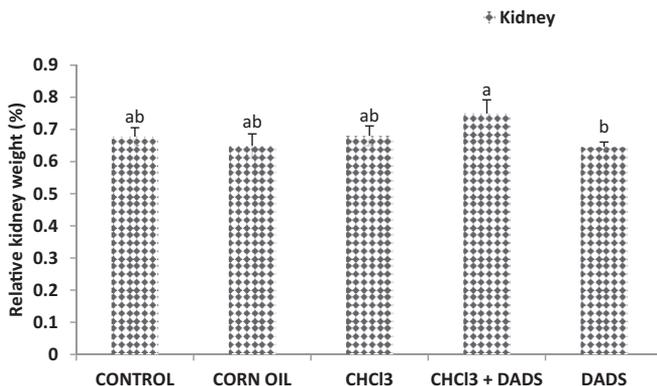## 3. Results

### 3.1. Effect of $CHCl_3$ administration and DADS treatment on relative kidney weight

Following $CHCl_3$ administration, there was no significant difference ($p > 0.05$) in the relative kidney weight compared with control group and/or DADS treated groups (Figure 1).

3.2. Effect of $CHCl_3$ administration and DADS treatment on hepatic expressions of NFkB

As represented in Figure 2, expressions of renal NFkB significantly increased ($p < 0.05$) following $CHCl_3$ administration compared with the control. However, treatment with DADS did not have any significant effect ($p > 0.05$).


Fig. 1. Effect of $CHCl_3$ administration and DADS treatment on relative kidney weight. Values are expressed as mean ± standard error of mean (n = 5). Bars labeled with different superscript are statistically significant ($p < 0.05$). $CHCl_3$ = trichloromethane; DADS = diallyl disulfide.
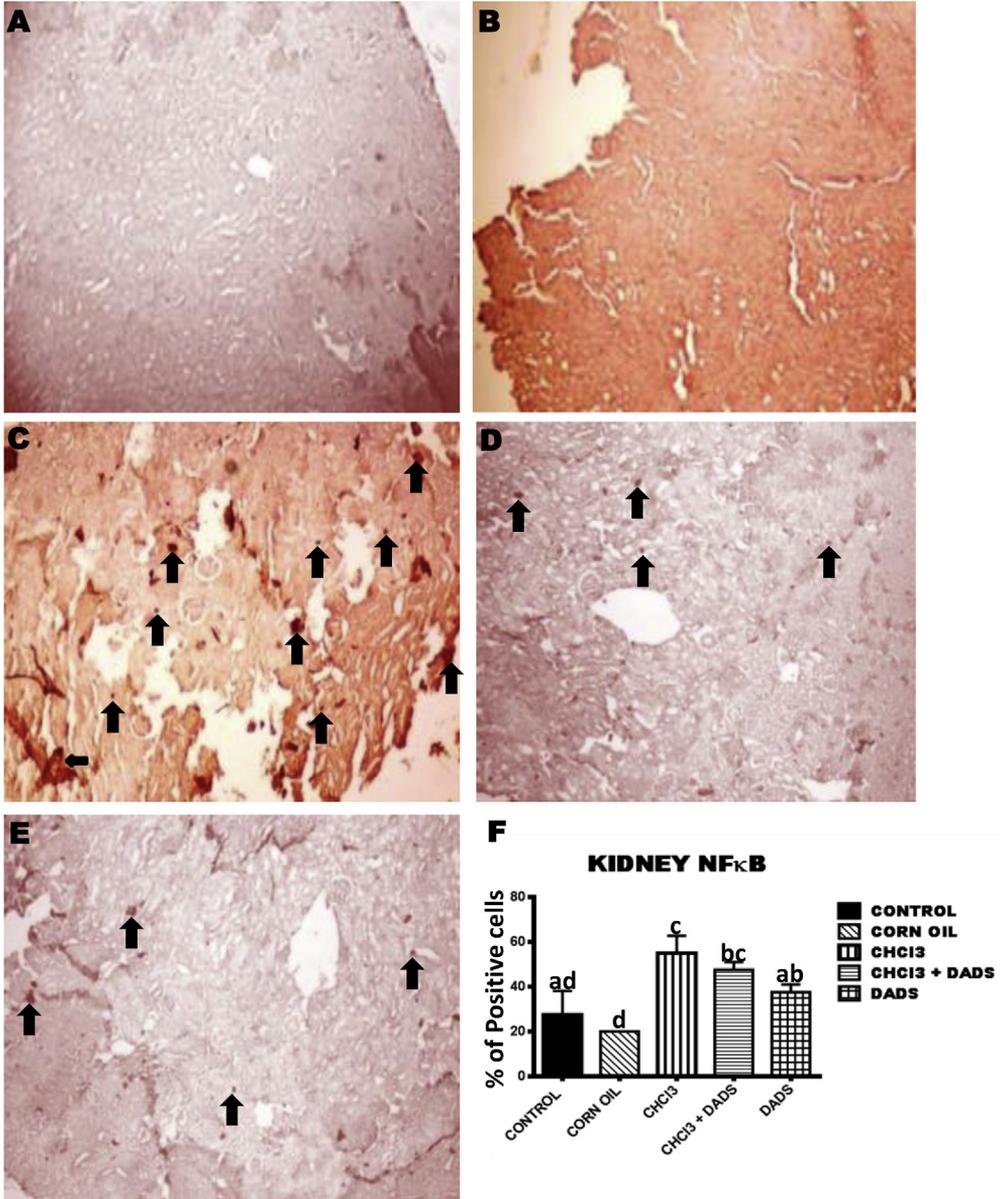
Fig. 2. Effects of DADS on $CHCl_3$-induced NFkB activation. Representative photographs of immunohistochemical analysis of NFkB in kidney sections of (A) control, (B) cornoil, (C) $CHCl_3$, (D) $CHCl_3$ + DADS, (E) DADS. The black arrows point to NFkB positive cells. (F) Each bar represents mean ± SEM of three (3) rats per group. Bars labeled with different superscript are statistically significant ($p < 0.05$). $CHCl_3$ = trichloromethane; DADS = diallyl disulfide.

3.3. Effect of $CHCl_3$ administration and DADS treatment on hepatic expressions of p53

Expressions of kidney p53 were depicted in Figure 3. Following $CHCl_3$ administration, level of p53 expressions significantly decreased ($p < 0.05$) compared with control. The expressions were however significantly increased ($p < 0.05$) following DADS treatment.
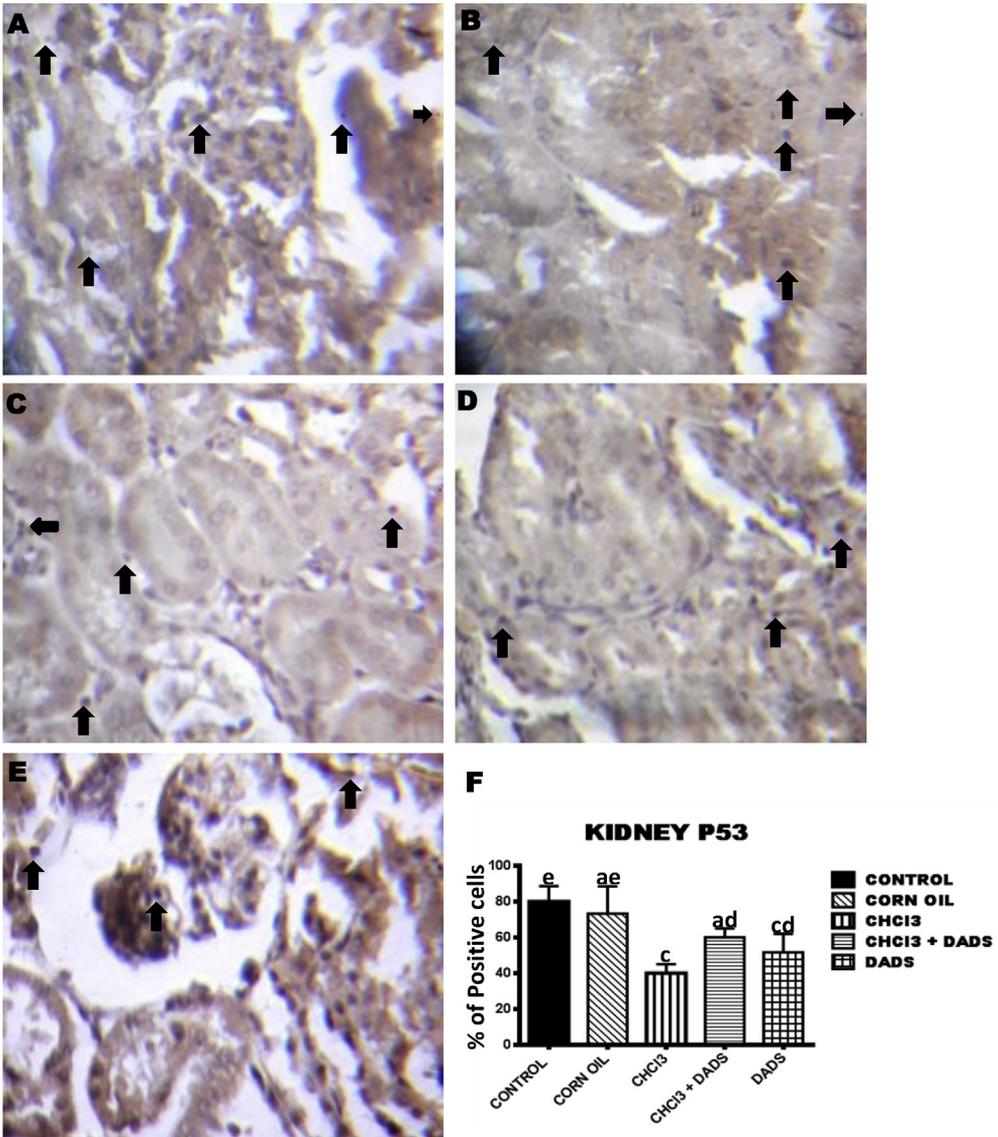
Fig. 3. Effects of DADS on $CHCl_3$-induced p53 expressions. Representative photographs of immunohistochemical analysis of p53 in kidney sections of (A) control, (B) cornoil, (C) $CHCl_3$, (D) $CHCl_3$ + DADS, (E) DADS. The black arrows point to p53 positive cells. (F) Each bar represents mean $\pm$ SEM of three (3) rats per group. Bars labeled with different superscript are statistically significant ($p < 0.05$). $CHCl_3$ = trichloromethane; DADS = diallyl disulfide.

3.4. Effects of DADS on $CHCl_3$-induced hepatic cellular apoptosis

Administrations of $CHCl_3$ significantly increased ($p < 0.05$) the number of apoptotic cells (TUNEL positive cells) compared with control (Figure 4). However, following DADS concomitant treatment, the number of apoptotic cells (TUNEL positive cells) was significantly ($p < 0.05$) reduced when compared with $CHCl_3$ group.
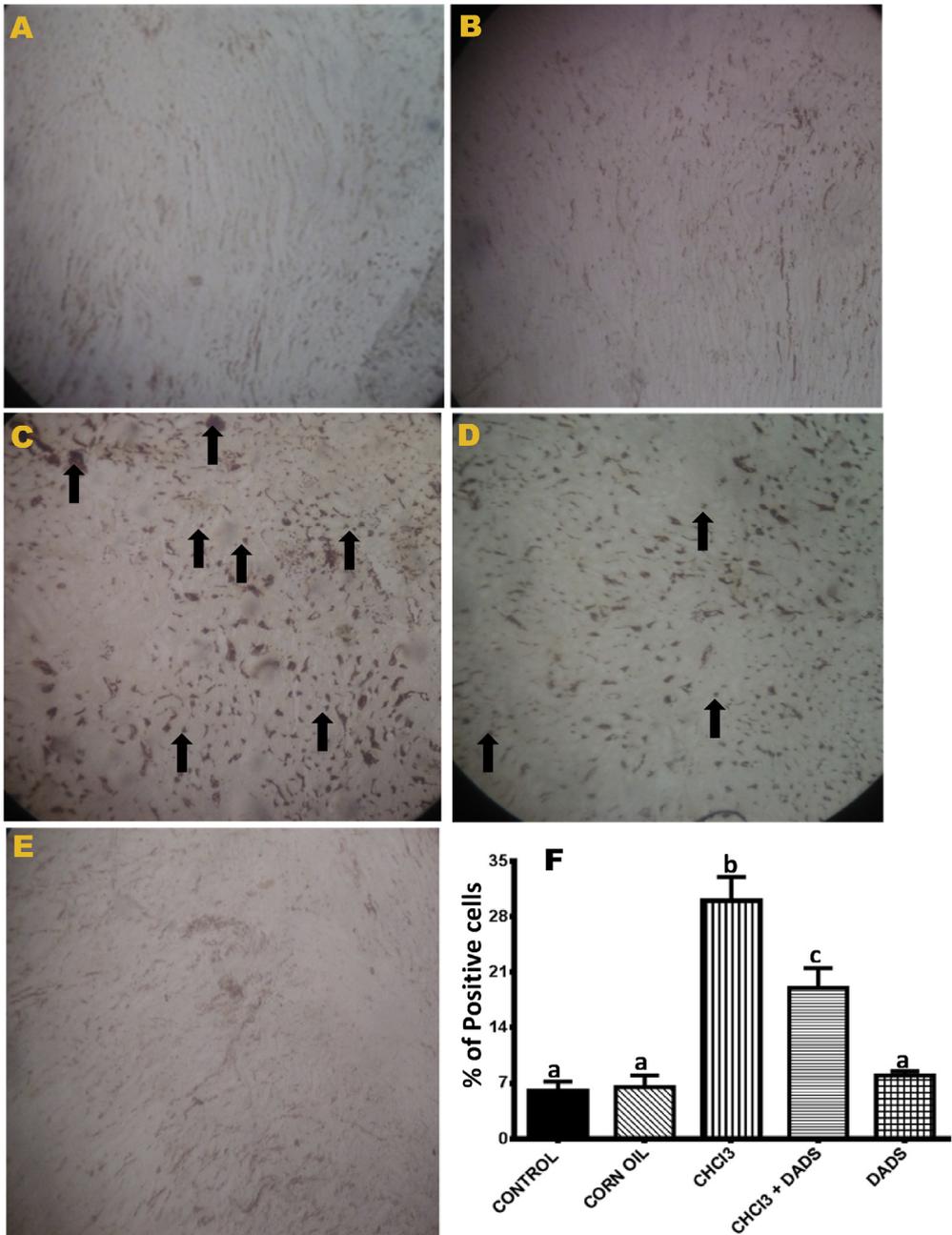
Fig. 4. Effects of DADS on CHCl$_3$-induced renal cellular apoptosis. Representative photographs of TUNEL assay performed on kidney sections of (A) control, (B) cornoil, (C) CHCl$_3$, (D) CHCl$_3$ + DADS, (E) DADS. The black arrows point to the apoptotic cells (TUNEL-positive cells). (F) Values are expressed as mean ± standard error of mean (n = 3). Bars labeled with different superscript are statistically significant (p < 0.05). CHCl$_3$ = trichloromethane; DADS = diallyl disulfide.

3.5. Effect of CHCl$_3$ administration and DADS treatment on kidney MDA concentration

No significant difference (p > 0.05) in kidney MDA was recorded following administration of CHCl$_3$ compared with control and/or DADS treated groups (Figure 5).

3.6. Effect of CHCl$_3$ administration and DADS treatment on kidney H$_2$O$_2$ level

CHCl$_3$ administration significantly (p < 0.05) increase the level of H$_2$O$_2$ (Figure 6), but was restored to level comparable with the control when concomitantly treated with DADS (Fig. 6).

3.7. Effect of CHCl$_3$ administration and DADS treatment on kidney NO concentration

NO concentration was also significantly (p < 0.05) increased by CHCl$_3$ administration (Figure 7) compared with control, and DADS co-administration was able to significantly reduced the concentration (Fig. 7).

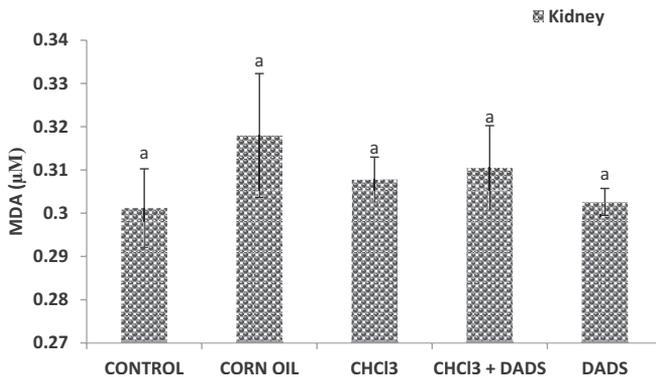### 3.8. Effect of CHCl$_3$ administration and DADS treatment on level of kidney GSH

A significant increase (p < 0.05) in the level of GSH was recorded following CHCl$_3$ administration (Figure 8). DADS intervention was however ineffective (Fig. 8).

3.9. Effect of CHCl$_3$ administration and DADS treatment on activity of kidney GPx

For GPx (Figure 9), administration of CHCl$_3$ did not have significant (p > 0.05) effect on the enzyme compared with control, but co-administration of DADS was effective as it significantly (p < 0.05) increased its activity (Fig. 9).

3.10. Effect of CHCl$_3$ administration and DADS treatment on activity of kidney CAT

CAT activity was significantly decreased (p < 0.05) by the administration of CHCl$_3$ compared with control (Figure 10). Concomitant treatment with DADS significantly increased (p < 0.05) the activity to level comparable with control (Fig. 10).

Fig. 5. Effect of CHCl$_3$ administration and DADS treatment on kidney MDA concentration. Values are expressed as mean ± standard error of mean (n = 5). Bars labeled with different superscript are statistically significant (p < 0.05). CHCl$_3$ = trichloromethane; DADS = diallyl disulfide.
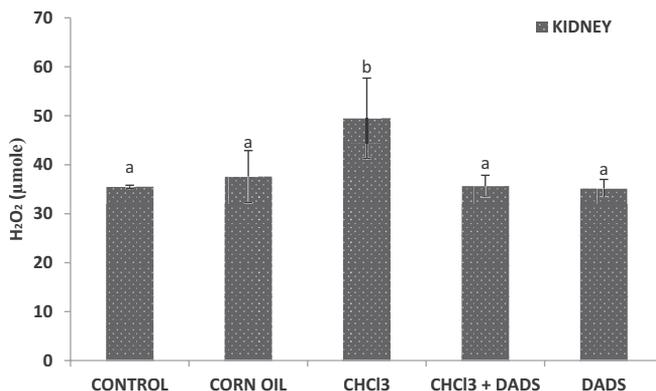
Fig. 6. Effect of $CHCl_3$ administration and DADS treatment on kidney H_2O_2 concentration. Values are expressed as mean ± standard error of mean (n = 5). Bars labeled with different superscript are statistically significant (p < 0.05). $CHCl_3$ = trichloromethane; DADS = diallyl disulfide.
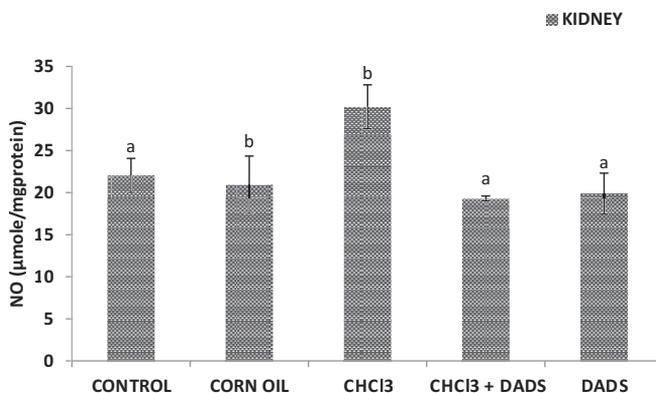
Fig. 7. Effect of $CHCl_3$ administration and DADS treatment on kidney NO concentration. Values are expressed as mean ± standard error of mean (n = 5). Bars labeled with different superscript are statistically significant (p < 0.05). $CHCl_3$ = trichloromethane; DADS = diallyl disulfide.
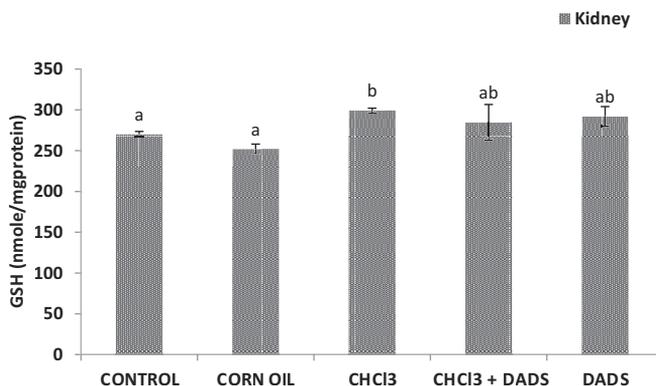

Fig. 8. Effect of $CHCl_3$ administration and DADS treatment on kidney GSH concentration. Values are expressed as mean ± standard error of mean (n = 5). Bars labeled with different superscript are statistically significant (p < 0.05). $CHCl_3$ = trichloromethane; DADS = diallyl disulfide.

Fig. 9. Effect of $CHCl_3$ administration and DADS treatment on kidney GPx activity. Values are expressed as mean $\pm$ standard error of mean (n = 5). Bars labeled with different superscript are statistically significant (p < 0.05). $CHCl_3$ = trichloromethane; DADS = diallyl disulfide.
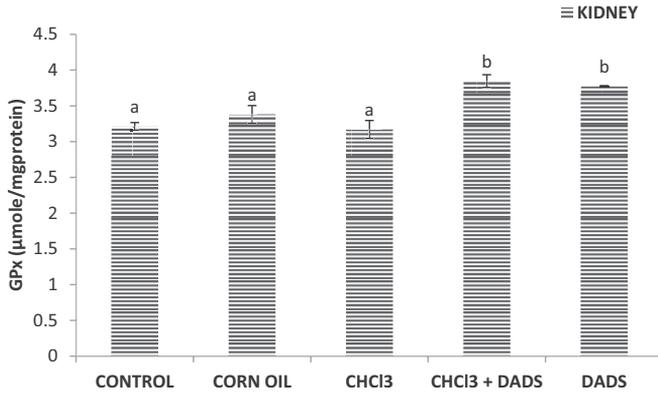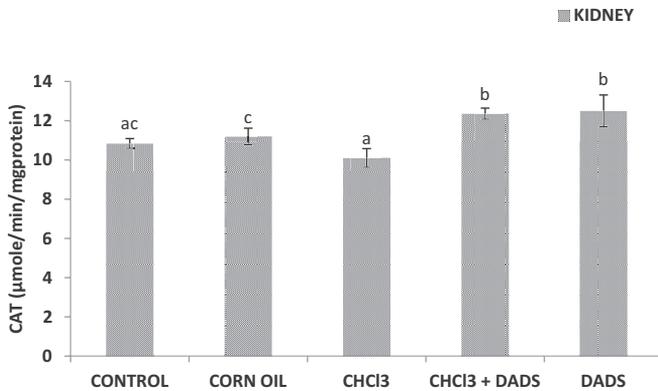

Fig. 10. Effect of $CHCl_3$ administration and DADS treatment on kidney CAT activity. Values are expressed as mean $\pm$ standard error of mean (n = 5). Bars labeled with different superscript are statistically significant (p < 0.05). $CHCl_3$ = trichloromethane; DADS = diallyl disulfide.

3.11. Effects of DADS treatment on kidney histopathology of rats administered $CHCl_3$ and treated with DADS

For the control, corn oil, and DADS only groups, no visible lesions were seen (Figure 11). Following $CHCl_3$ administration, there was a severe interstitial congestion of the kidney especially at the renal cortex, while treatment with DADS revealed few foci of mild interstitial hemorrhage (Fig. 11).

4. Discussion

The present study investigated the chemotherapeutic effect of DADS in $CHCl_3$-induced nephrotoxicity in male wistar rats. Following the administration of 200 mg/kg $CHCl_3$ five days a week for three weeks, no significant effect was seen on the relative kidney weight compared with control and other groups (Fig. 1). Similarly, in a study conducted by Larson et al. [34], the relative kidney weight only increased after three weeks of administration of 180 mg/kg/day of $CHCl_3$.

NFkB is a transcription factor that has been reported to promote carcinogenesis by regulating the expression of genes that are involved in cell proliferation, metastasis and apoptosis [44–46]. In the cytoplasm, NFkB is rendered inactive by being sequestered to its inhibitor called IkB. Upon exposure of the cell to toxicants, a cascade of reactions ensue which leads to the phosphorylation of IkB by IKK, a
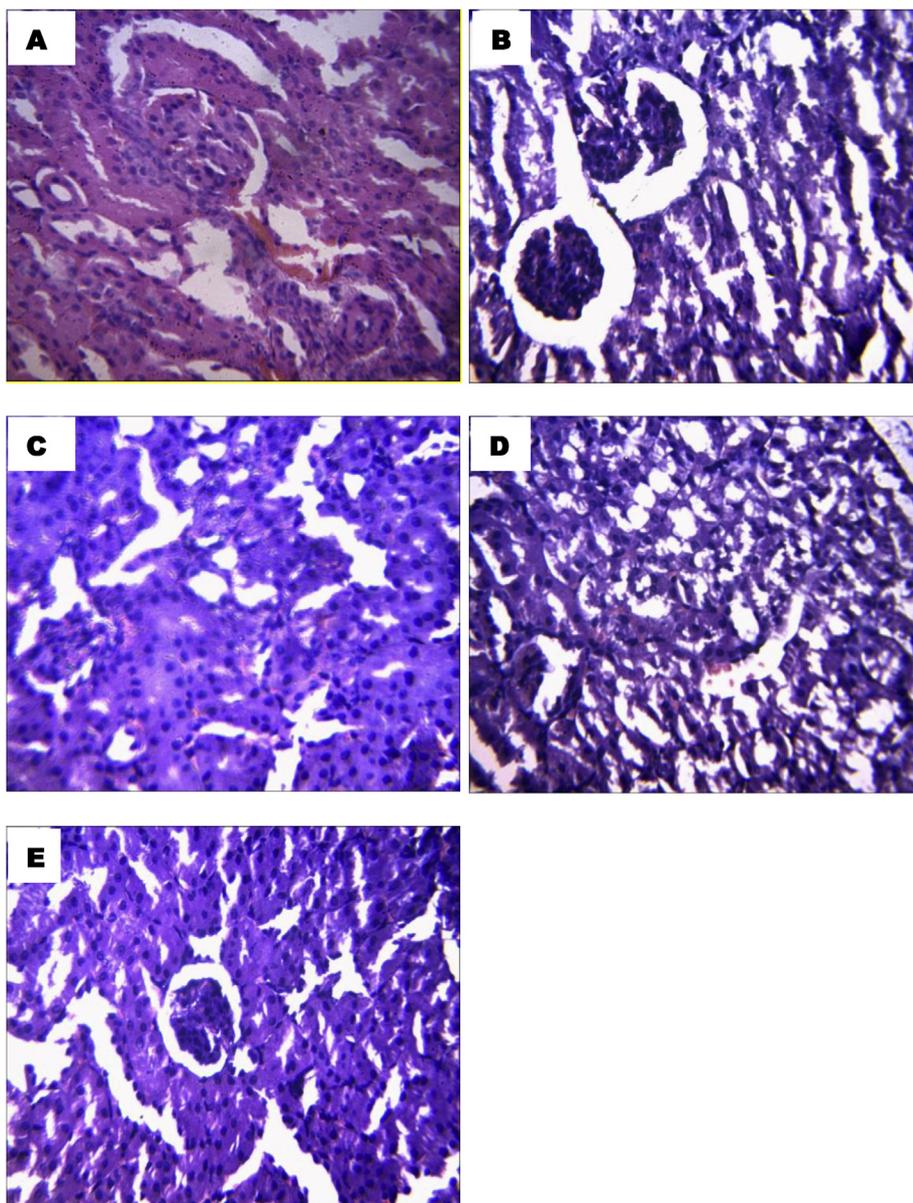
Fig. 11. Effects of DADS on CHCl$_3$-induced kidney histopathological alterations (100x). Control (A): No visible lesion, Corn oil (B): No visible lesion, CHCl$_3$ (C): There is a severe interstitial congestion of the kidney especially at the renal cortex, CHCl$_3$ + DADS (D): There are few foci of mild interstitial hemorrhage, DADS (E): No visible lesion. CHCl$_3$ = trichloromethane; DADS = diallyl disulfide.

kinase, and subsequent ubiquitination and degradation, causing the separation of NFkB and its translocation into the nucleus where it coordinate the expressions of genes that participate in inflammation and carcinogenicity. While NF-kB has become a promising target for anticancer therapy, the complexity of NFkB regulation has made it challenging to develop agents to suppress its activation [47]. In this study, the significant increase in the expressions of renal NFkB is an indication of TCM-induced activation, thus suggesting its role in renal toxicity.

p53 is a transcription factor that activates genes that function in cellular responses to DNA damage. It plays a critical role in controlling cell cycle arrest and apoptosis [48]. p53 gene stops cell cycle in G1 phase when there is DNA damage or a base mismatch. Failure of the damage to repair itself causes the cell to undergo apoptosis, which may occur at any stage of the cell cycle [49]. Apoptosis is a form of cell death where cells actively participate in their own destruction, a process characterized by specific morphological and biochemical changes and also by alterations of genomic expression [50,51]. Being a key component in the response to cellular stress, p53 serves as a major obstruction for carcinogenesis [52]. Significant decrease in the expressions of p53 recorded in this study following TCM administration may be attributed to a role in kidney cancer [53] and excessive apoptosis, which agrees with the studies of Zhu et al. [54] who reported low p53 expressions in cisplastin-induced nasopharyngeal cancer, and Ahmed et al. [55] who also reported low expressions following nicotine administration. Furthermore, increase in the expressions of p53 by DADS co-administrations can be attributed to its renal-protective and anticancer properties as reported by Nakagawa et al. [22], Guyonnet et al. [23], and Pedraza-Chaverri et al. [25].

Apoptosis, a process often referred to as programmed cell death, occurs when cells have developed irreparable defects that can ultimately lead to cancer. p53 is a well-known tumor suppressor protein that can prevent cells from becoming malignant via initiation of cell cycle arrest [56,57]. It is a key regulator of apoptosis and carcinogenesis [58—62]. The significant increase in apoptosis (TUNEL positive cells) following $CHCl_3$ administration is an indication of damage to the kidney cells [8], causing the renal cells to undergo apoptosis in a failed attempt to repair the cells. This may also explain the low expressions of p53 recorded in this study, which may have been overwhelmed in an attempt to ameliorate $CHCl_3$ toxicity. In similar findings by Lee et al. [63], administration of carbon tetrachloride (CCl_4) to rats significantly increased the number TUNEL positive cells. Also, in this study, the resulting significant decrease following DADS co-administration with $CHCl_3$ explains its antioxidant, anti-apoptotic and renal-protective effects as also reported by Lee et al. [63], as well as Kim et al., [64] and Kim et al., [27].

Quantification of thiobarbituric acid (TBARS) is majorly used to assess lipid peroxidation and indirectly, oxidative stress *in vitro* and *in vivo* [65]. Oxidation of lipids causes disruption of the membrane bilayers that are rich in unsaturated fatty acids, following their attack by free radicals in an attempt to become paired and stable, compromising cell integrity, and leading to leakage of cellular content from the damaged organ into the blood stream [66,67]. In this study, no significant effect was recorded for kidney MDA (Fig. 2) following administration of $CHCl_3$. The capability of the kidney antioxidant defense system to protect against free radical attack may be responsible for this.

The hazardous chemical effects of H_2O_2 molecules are as a result of direct activity, emanating from their oxidizing properties, and the indirect activity where they serve as a source for more toxic species, like hydroxyl radicals and hypochlorous acid [68]. The significant high level of H_2O_2 (Fig. 3) is an indication of tissue damage [69]. However, the significant decrease following DADS intervention is an indication of its antioxidant and free radical mopping properties [63].

NO is a potent pro-inflammatory mediator, a low level is known to play an important role in cellular signaling under normal physiological condition. On the other hand, excessive production in the cell can lead to generation of peroxynitrite which subsequently damage the tissue [36,70]. Thus, high level of hepatic NO reported in this study (Fig. 4) may be an indication of nitrosative stress and renal inflammation following $CHCl_3$ administration. Following DADS co-treatment, the resulting significant decrease in the level of NO (Fig. 4) suggests its anti-inflammatory and anti-nitrosative potentials [71—73].

Oxidative stress is characterized by increase in the levels of free radicals due to insufficient antioxidant defense [74]. It has been documented in clinical and experimental studies to play a key role in the etiology of many diseases including cancer, rheumatoid arthritis, diabetes mellitus, cardiovascular diseases, and neurological disorders such as Parkinson and Alzheimer [75]. The body has its antioxidant systems to prevent the production of reactive oxygen or nitrogen species and the ravaging and destructive effects they can cause. The most important intracellular antioxidant defense enzymes are catalase, glutathione peroxidase superoxide dismutase [76] and non-enzymatic antioxidants like reduced glutathione [77]. The significant increase in the level of kidney GSH as well as significant and non-significant decrease in CAT and GPx activities respectively following $CHCl_3$ administration is an

indication of free radical generation (H$_2$O$_2$), which the endogenous antioxidant enzymes were responsive to. Antioxidant potentials of DADS was exerted which resulted to the restoration of the renal CAT [63,78–80] and GPx [25,63,81,82] activities.

The severe interstitial congestion of the kidney especially at the renal cortex is an evidence of CHCl$_3$ toxicity on the renal cells. However, the few foci of mild interstitial hemorrhage following DADS treatment are indications of conferred protection to some extent, against the toxicity.

5. Conclusion

In conclusion, protection by DADS against TCM-induced renal-toxicity may therefore be via suppressions of NFkB activation, oxidative stress and apoptosis in rats.

Source of funding

None.

Conflict of interest

None.

References

[1] Lewis RJ. Hawley's condensed chemical dictionary. 12th ed. New York: Van Nostrand Reinhold; 1993. p. 266–7.
[2] Craun GF. Safety of water disinfection: balancing chemical and microbial risks. Washington DC: ILSI Press; 1993.
[3] Deinzer M, Schaumburg F, Klein E. Environmental health sciences center task force review on halogenated organics in drinking water. Environ Health Perspect 1978;24:209–39.
[4] Abbassi R, Chamkhia N, Sakly M. Chloroform-induced oxidative stress in rat liver: implication of metallothionein. Toxicol Ind Health 2010;26(8):487–96.
[5] HazDat. Agency for toxic substance and diseaseregistry. 2001. Atlanta, GA.
[6] International Agency for Research on Cancer. Monographs on the evaluation of carcinogenic risks to humans. Some chemicals that cause tumours of the kidney or urinary bladder in rodents and some other substances, vol. 73; 1999.
[7] Constan AA, Sprankle CS, Peters JM, Kedderis GL, Everitt JI, Wong BA, et al. Metabolism of chloroform by cytochrome P450 2E1 is required for induction of toxicity in the liver, kidney, and nose of male mice. Toxicol Appl Pharmacol 1999;160: 120–6.
[8] International Life Sciences Institute. An evaluation of EPA's proposed guidelines for carcinogen risk assessment using chloroform and dichloroacetate as case studies: report of an expert panel. Washington, DC: ILSI Health and Environmental Sciences Institute; November 1997.
[9] US EPA. Summary of new data on trihalomethanes (THMS) for the notice of availability. Draft. 1997.
[10] US EPA. Health risk assessment/characterization of the drinking water disinfection byproduct chloroform. Washington, DC: Prepared for Health and Ecological Criteria Division, Office of Science and Technology; November 4;1998. Prepared by Toxicology Excellence for Risk Assessment, cincinnati, OH, under purchase Order No. 8W-0767-NTLX.
[11] De Bruyn WJ, Shorter JA, Davidovits P, Worsnop DR, Zahniser MS, Kolb CE. Uptake of haloacetyl and carbonyl halides by water surfaces. Environ Sci Technol 1995;29:1179–85.
[12] Schneider W, Diller W, Phosgene. In: Elvers B, Hawkins S, Schulz G, editors. Ullmann's encyclopedia of industrial chemicals. Fifth, completely revised edition; 1991.
[13] Noort D, Hulst AG, Fidder A, van Gurp RA, de Jong LPA, Benschop HP. In vitro adduct formation of phosgene with albumin and hemoglobin in human blood. Chem Res Toxicol 2000;13:719–26.
[14] Pereira MA, Chang LW. Binding of chemical carcinogens and mutagens to rat hemoglobin. Chem Biol Interact 1981;33: 301–5.
[15] Pereira MA, Chang LW, Ferguson JL, Couri D. Binding of chloroform to the cysteine of hemoglobin. Chem Biol Interact 1984; 51:115–24.
[16] Pohl LR, Bhooshan B, Whittaker NF, Krishna G. Phosgene: a metabolite of chloroform. Biochem Biophys Res Comm 1977; 79:684–91.
[17] Pohl LR, Martin JL, George JW. Mechanism of metabolic activation of chloroform by rat liver microsomes. Biochem Pharmacol 1980;29:3271–6.
[18] Pohl LR, Branchflower RV, Highet RJ, Martin JL, Nunn DS, Monks TJ, et al. The formation of diglutathionyl dithiocarbonate as a metabolite of chloroform, bromotrichloromethane, and carbon tetrachloride. Drug Metab Dispos 1981;9:334–9.
[19] World Health Organization. Guidelines for drinking-water quality. Second edition. Addendum to volume 2. Geneva: World Health Organization; 1998. p. 255–75. Health criteria and other supporting information. Chloroform.
[20] Shin JH, Lee CW, Oh SJ, Yun J, Kang MR, Han SB, et al. Hepatoprotective effect of aged black garlic extract in rodents. Toxicol Res 2014;30:49–54.
[21] Ariga T, Seki T. Antithrombotic and anticancereffects of garlic-derived sulfur compounds: a review. Biofactors 2006;26: 93–103.

[22] Nakagawa H, Tsuta K, Kiuchi K, Senzaki H, Tanaka K, Hioki K, et al. Growth inhibitory effects of diallyl disulfide on human breast cancer cell lines. Carcinogenesis 2001;22(6):891—7.
[23] Guyonnet D, Belloir C, Suschetet M, Siess MH, Le Bon AM. Mechanisms of protection against aflatoxin B(1) genotoxicity in rats treated by organosulfur compounds from garlic. Carcinogenesis 2002;23(8):1335—41.
[24] Manesh C, Kuttan G. Alleviation of cyclophosphamide-induced urotoxicity by naturally occurring sulphur compounds. J Exp Clin Canc Res 2002;21(4):509—17.
[25] Pedraza-Chaverrí J, González-Orozco AE, Maldonado PD, Barrera D, Medina-Campos ON, Hernández-Pando R. Diallyl disulfide ameliorates gentamicin-induced oxidative stress and nephropathy in rats. Eur J Pharmacol 2003;473(1):71—8.
[26] Fukao T, Hosono T, Misawa S, Seki T, Ariga T. The effects of allyl sulfides on the induction of phase II detoxification enzymes and liver injury by carbon tetrachloride. Food Chem Toxicol 2004;42(5):743—9.
[27] Kim SH, Lee IC, Ko JW, Shin IS, Moon C, Kim SH, et al. Mechanism of protection by diallyl disulfide against cyclophosphamide-induced spermatotoxicity and oxidative stress in rats. Mol Cell Toxicol 2016;12:301—12.
[28] Belman S, Solomon J, Segal A, Block E, Barany G. Inhibition of soybean lipoxygenase and mouse skin tumor promotion by onion and garlic components. J Biochem Toxicol 1989;4:151—60.
[29] Sundaram SG, Milner JA. Impact of organosulfur components in garlic on canine mammary tumor cells in culture. Cancer Lett 1993;74:85—90.
[30] Morris CR, Chen SC, Zhou L, Schopfer LM, Ding X, Mirvish SS. Inhibition by allyl sulfides and phenethyl isothiocyanate of methyl-n-pentylnitrosamine depentylation by rat esophageal microsomes, human and rat CYP2E1, and rat CYP2A3. Nutr Canc 2004;48:54—63.
[31] Druesne N, Pagniez A, Mayeur C, Thomas M, Cherbuy C, Duee PH, et al. Diallyl disulfide (DADS) increases histone acetylation and p21 (waf1/cip1) expression in human colon tumor cell lines. Carcinogenesis 2004;25:1227—36.
[32] Filomeni G, Aquilano K, Rotilio G, Ciriolo MR. Reactive oxygen species-dependent c-Jun NH2-terminal kinase/c-Jun signaling cascade mediates neuroblastoma cell death induced by diallyl disulfide. Cancer Res 2003;63:5940—9.
[33] Wen J, Zhang Y, Chen X, Shen L, Li GC, Xu M. Enhancement of diallyl disulfide-induced apoptosis by inhibitors of MAPKs in human HepG2 hepatoma cells. Biochem Pharmacol 2004;68:323—31.
[34] Larson JL, Wolf DC, Mery S, Morgan KT, Butterworth BE. Kidneys and nasal passages of female F-344 rats, induced by chloroform administered by gavage. Food Chem Toxicol 1995;33(6):443—56.
[35] National Research Council. Guide for the care and use of laboratory animals. Washington, DC: National Academy Press; 1996.
[36] Ajayi BO, Adedara AI, Farombi EO. Benzo(a)pyrene induces oxidative stress, pro-inflammatory cytokines, expression of nuclear factor-kappa B and deregulation of wnt/beta-catenin signaling in colons of BALB/c mice. Food Chem Toxicol 2016; 95:42—51.
[37] Buege JA, Aust SD. Microsomal lipid peroxidation. Methods Enzymol 1978;52:302—10.
[38] Wolff SP. Ferrous ion oxidation in the presence of ferric ion indicator xylenol orange for measurement of hydroperoxides. Methods Enzymol 1994;233:182—9.
[39] Green LC, Wagner DA, Glogowski J, Skiper PL, Wishnock JS, Tannenbaum SR. Analysis of nitrate, nitrite and [15 N] nitrate in biological fluids. Anal Biochem 1982;126:131—8.
[40] Moron MS, Depierre JW, Mannervik B. Levels of glutathione, glutathione reductase and glutathione S-transferase activities in rat lung and liver. Biochim Biophys Acta 1979;582:67—78.
[41] Rotruck JT, Pope AL, Ganther HE, Swanson AB, Hafeman DG, Hoekstra WG. Selenium: biochemical role as a component of glutathione peroxidase. Science 1973;179:588—90.
[42] Sinha AK. Colorimetric assay of catalase. Anal Biochem 1972;47:389—94.
[43] Gornall AG, Bardawill CJ, David MM. Determination of serum protein by biuret method. J Biol Chem 1949;117:751—66.
[44] Erstad DJ, Cusack Jr JC. Targeting the NF-kappaB pathway in cancer therapy. Surg Oncol Clin 2013;22:705—46.
[45] Hoesel B, Schmid JA. The complexity of NF-kappaB signaling in inflammation and cancer. Mol Canc 2013;12:86.
[46] Jing H, Lee S. NF-kappaB in cellular senescence and cancer treatment. Mol Cell 2014;37:189—95.
[47] Saud SM, Li W, Gray Z, Matter MS, Colburn NH, Young MR, et al. Diallyl disulfide (DADS), a constituent of garlic, inactivates NF-kB and prevents colitis-induced colorectal cancer by inhibiting GSK-3β. Cancer Prev Res 2016;9:607—15.
[48] Vousden K, Lane D. p53 in health and disease. Nat Rev Mol Cell Biol 2007;8:275—83.
[49] Wei Y, Cao X, Ou Y, Lu J, Xing C, Zheng R. SeO₂ induces apoptosis with down-regulation of Bcl-2 and up-regulation of p53 expression in both immortal human hepatic cell line and hepatoma cell line. Mutat Res 2001;490:113—21.
[50] Kajta K. Apoptosis in the central nervous system: mechanisms and protective strategies. Pol J Pharmacol 2004;56: 689—700.
[51] Philchenkov A. Caspases: potential targets for regulating cell death. J Cell Mol Med 2004;8:432—44.
[52] Haupt S, Berger M, Goldberg Z, Haupt Y. Apoptosis — the p53 network. J Cell Sci 2003;116:4077—85.
[53] National Cancer Institute. Carcinogenesis bioassay of chloroform. National tech. Inform. Service No. PB264018/AS. Bethesda, MD: National Cancer Institute; 1976.
[54] Zhu K, Jiang L, Chu Y, Zhang YS. Protective effect of selenium against cisplastin-induced nasopharyngeal cancer in male albino rats. Oncol Lett 2016;12:5068—74.
[55] Ahmed MA, Hassan KH, Hassanein KMA, Waly H. Role of vitamin C and selenium in attenuation of nicotine induced oxidative stress, p53 and Bcl2 expression in adult rat spleen. Pathophysiology 2014;21:211—7.
[56] Cell-matrix adhesion, cell-cell interactions, and malignancy. In: Streuli CH, Pelengaris S, Kahn M, editors. The molecular biology of cancer. Blackwell Publishing; 2006. p. 357—88.
[57] Vogelstein B, Kinzler KW. Cancer genes and the pathways they control. Nat Med 2004;10:789—99.
[58] Levine AJ, Momand J, Finlay CA. The p53 tumor suppressor gene. Nature 1991;351:453—6.
[59] Parant JM, Lozano G. Disrupting TP53 in mouse models of human cancers. Hum Mutat 2003;21(3):321—6.
[60] Chen Z, Trotman LC, Shaffer D, Lin HK, Dotan ZA, Niki M, et al. Crucial role of p53-dependent cellular senescence in suppression of Pten-deficient tumorigenesis. Nature 2005;436:725—30.
[61] Vousden KH, Prives C. p53 and prognosis: new insights and further complexity. Cell 2005;120(1):7—10.
[62] Pelengaris S, Khan M. In: Pelengaris S, Khan M, editors. The molecular biology of cancer. Blackwell Publ; 2006. p. 251—78.

[63] Lee IC, Kim SH, Baek HS, Moon C, Kang SS, Kim SH, et al. The involvement of Nrf2 in the protective effects of diallyl disulfide on carbon tetrachloride-induced hepatic oxidative damage and inflammatory response in rats. Food Chem Toxicol 2014;63:174–85.

[64] Kim SH, Lee IC, Baek HS, Shin IS, Moon C, Bae CS, et al. Mechanism for the protective effect of diallyl disulfide against cyclophosphamide acute urotoxicity in rats. Food Chem Toxicol 2014;64:110–8.

[65] Beltowski J, Wojcicka G, Gorny D, Marciniak A. The effect of dietary-induced obesity on lipid peroxidation, antioxidant enzymes and total plasma antioxidant capacity. J Physiol Pharmacol 2000;51:883–96.

[66] Somade OT, Olorode SK, Olaniyan TO, Faokunla O. Quercetin, a polyphenolic phytochemical prevents sodium azide-induced extrahepatic oxidative stress in rats. Cog Biol 2016;2:1200798.

[67] Somade OT, Adeniji KD, Adesina AA, Olurinde OJ. Oral acute toxicity study as well as tissues oxidative stress and histopathological disorders in edible camphor administered rats. Exp Toxicol Pathol 2017;69:99–108.

[68] Kohen R, Nyska A. Oxidation of biological systems: oxidative stress phenomena, antioxidants, redox reactions, and methods for their quantification. Toxicol Pathol 2002;30:620–50.

[69] Farombi EO, Adedara IA, Ajayi BO, Ayepola OR, Egbeme EE. Kolaviron, a natural antioxidant and anti-inflammatory phytochemical prevents dextran sulphate sodium-induced colitis in rats. Basic Clin Pharmacol Toxicol 2013;113(1):49–55.

[70] Ignarro LJ, Cirino G, Casini A, Napoli C. Nitric oxide as a signaling molecule in the vascular system: an overview. J Cardiovasc Pharmacol 1999;34:879–86.

[71] Indhira KR, Kumaravel P, Subash S, Sivaperumal R, Subramanian P. Protective effect of diallyl disulphide on hyperammonemic rats. J Pharm Res 2012;5:4–8.

[72] Chiang YH, Jen LN, Su HY, Lii CK, Sheen LY, Liu CT. Effects of garlic oil and two of its major organosulfur compounds,diallyl disulfide and diallyl trisulfide, on intestinal damage in rats injected with endotoxin. Toxicol Appl Pharmacol 2006;213:46–54.

[73] Chang HP, Chen YH. Differential effects of organosulfur compounds from garlic oil on nitric oxide and prostaglandin E2 in stimulated macrophages. Nutrition 2005;21:530–6.

[74] Mittler R. Oxidative stress, antioxidants and stress tolerance. Trends Plant Sci 2002;7:405–10.

[75] Valko M, Leibfritz D, Moncol J, Cronin MT, Mazur M, Telser J. Free radicals and antioxidants in normal physiological functions and human disease. Int J Biochem Cell Biol 2007;39:44–84.

[76] Altan N, Dincel AS, Koca C. Diabetes mellitus veoksidatif stres. Turkish J Biochem 2006;31:51–6.

[77] Tomlin CD. The E-pesticide manual. 10th ed. Surrey, UK: The British Crop Protection Council; 1994.

[78] Kim SH, Lee IC, Ko JW, Moon C, Kim SH, Shin IS, et al. Diallyl disulfide prevents cyclophosphamide-induced hemorrhagic cystitis in rats through the inhibition of oxidative damage, MAPKs, and NF-κB pathways. Biomol Ther 2015;23:180–8.

[79] Khatua TN, Dinda AK, Putcha UK, Banerjee SK. Diallyldisulfide ameliorates isoproterenol-induced cardiac hypertrophy activating mitochondrial biogenesis via eNOS-Nrf2-Tfam pathway in rats. Biochem Biophy Rep 2016;5:77–88.

[80] Ko JW, Park SH, Shin NR, Shin JY, Kim JW, Shin IS, et al. Protective effect and mechanism of action of diallyl disulfide against acetaminophen-induced acute hepatotoxicity. Food Chem Toxicol 2017;109:28–37.

[81] Ko JW, Shin JY, Kim JW, Park SH, Shin NR, Lee IC, et al. Protective effects of diallyl disulfide against acetaminophen-induced nephrotoxicity: a possible role of CYP2E1 and NF-κB. Food Chem Toxicol 2017;102:156–65.

[82] Liu CT, Hsu TW, Chen KM, Tan YP, Lii CK, Sheen LY. The antidiabetic effect of garlic oil is associated with ameliorated oxidative stress but not ameliorated level of pro-inflammatory cytokines in skeletal muscle of streptozotocin-induced diabetic rats. J Trad Comp Med 2012;2:135–44.